AGU PUBLICATIONS

Geophysical Research Letters

RESEARCH LETTER
10.1002/2014GL062531

Key Points:
- Increase in diurnal and interdiurnal variability of European summer temperatures
- Role of land-air interactions, cloud processes, and large-scale dynamics
- Possibility to reduce future uncertainties through observational constraints

Supporting Information:
- Figures S1–S5 and Table S1

Correspondence to:
J. Cattiaux,
julien.cattiaux@meteo.fr

Citation:
Cattiaux, J., H. Douville, R. Schoetter, S. Parey, and P. Yiou (2015), Projected increase in diurnal and interdiurnal variations of European summer temperatures, *Geophys. Res. Lett.*, *42*, doi:10.1002/2014GL062531.

Received 13 NOV 2014
Accepted 14 JAN 2015
Accepted article online 16 JAN 2015

Projected increase in diurnal and interdiurnal variations of European summer temperatures

J. Cattiaux[1], H. Douville[1], R. Schoetter[1], S. Parey[2], and P. Yiou[3]

[1]CNRM-GAME, UMR 3589 CNRS/Météo-France, Toulouse, France, [2]EDF/R&D, Chatou, France, [3]LSCE/IPSL, UMR 8212 CEA/CNRS/UVSQ, Gif-sur-Yvette, France

Abstract Beyond the mean warming, climate change may modify the temperature variability, with consequences on extreme events causing societal and environmental impacts. Here we assess future changes in both the interdiurnal variability (ITV) and diurnal range (DTR) of European summer temperatures based on Fifth Phase of the Coupled Model Intercomparison Project projections under three 21st century scenarios. Both indices are projected to increase, with a rather good model agreement on the sign, while uncertainties remain on the amplitude. Extremely high day-to-day and diurnal temperature variations are expected to occur more frequently. Across models and scenarios, ITV and DTR increases vary primarily as functions of the decrease in surface evapotranspiration linked to the European summer drying. They are also partly explained by changes in the atmospheric dynamics and the surface cloud radiative effect. Model-dependent degrees of control of (i) ITV and DTR by mean temperature and (ii) surface evapotranspiration by soil moisture appear as helpful metrics to reduce future uncertainties in ITV and DTR projections.

1. Introduction

Global warming affects both the mean climate and its variability. Changes in climate variability, particularly in short-term variations responsible for extreme weather events, may induce the greatest socioeconomic and environmental impacts. Assessing such changes therefore represents a crucial challenge for both scientific and adaptation communities. In Europe, increases in summer temperature variability have been recently observed at both intraseasonal and interannual timescales [*Parey et al.*, 2010, 2013; *Yiou et al.*, 2009], and *Schär et al.* [2004] claimed that it contributed to the spectacular heat wave of summer 2003. Such increases have also been suggested in regional [*Fischer and Schär*, 2009; *Fischer et al.*, 2012; *Kjellström et al.*, 2007] and global [*Cattiaux et al.*, 2012; *Sillmann et al.*, 2013] climate projections for the 21st century, albeit with large intermodel discrepancies. Land-atmosphere processes have often been argued to be the prominent contributor to these increases in the European summer temperature variability, through the reduced evaporative fraction of surface heat fluxes by the long-term soil drying [*Seneviratne et al.*, 2006; *Zampieri et al.*, 2009]. Other potential processes, such as changes in large-scale atmospheric dynamics and/or cloud processes affecting the radiative budget, have been less documented. *Cattiaux et al.* [2012] nevertheless suggested that the increase in interannual variability could be partially explained by the atmospheric dynamics.

Also less documented are the changes in the two kinds of short-term temperature variability which we focus on in this paper: the variations within 1 day (diurnal temperature range (DTR)) and the variations from one day to the next one (interdiurnal temperature variability (ITV)). Among other impact communities [e.g., *Lobell*, 2007], these rapid variations represent key issues for energy providers since they can cause sudden surges in electricity demand, especially in a world of growing demand for air conditioning systems. We base our analysis on climate simulations provided by modeling groups participating to the Fifth Phase of the Coupled Model Intercomparison Project (CMIP5). ITV and DTR are determined by many interacting processes; the aim of this paper is not to fully evaluate the representation of these processes in CMIP5 models, but to document the projected changes in ITV and DTR with the associated uncertainties. Two recent studies by *Kim et al.* [2013] and *Lindvall and Svensson* [2014] investigated, respectively, ITV and DTR in subsets of CMIP5 simulations at the global scale: interestingly, decreases in both indices are expected in most land regions and seasons, except in Europe and in summer. While *Kim et al.* [2013] did not investigate the origins of the projected increase in the European summer ITV, *Lindvall and Svensson* [2014]

associated the DTR increase with reductions in the cloud radiative effect, the evaporative fraction, and the concentration of anthropogenic aerosols.

Here we assess the projected changes in European summer ITV and DTR based on a larger CMIP5 ensemble (section 3). Beyond the mean increase, we investigate changes in the distribution and extremes. Then we disentangle the contributions of large-scale atmospheric dynamics, soil drying, and cloudiness reduction and explore the possibility of reducing future model uncertainties through observational constraints. Data, methods, and computations of ITV and DTR indices are described in section 2, and conclusions are drawn in section 4.

2. Data and Indices of Variability

2.1. Data

We use outputs from 34 CMIP5 models (Table S1 in the supporting information), but depending on the data availability, not all models are included in all diagnostics of this paper. We focus on the summer season which we define as the June, July, August, and September months (JJAS). Models are evaluated by comparing their historical simulations with observations over the period 1979–2008. Future changes are assessed from differences between 1979–2008 and 2070–2099 in future projections, for which we use three distinct scenarios, namely the 2.6, 4.5, and 8.5 W/m^2 Representative Concentration Pathways (hereafter RCP2.6, RCP4.5, and RCP8.5). Historical simulations ending in 2005 were arbitrarily completed by corresponding RCP8.5 ones over the period 2006–2008 (scenarios are indistinguishable over this short period). For practical reasons, we only consider one realization per model and per experiment (*r1i1p1* in CMIP5 standards). We nevertheless account for the internal variability by also conducting the analyses for the 10 historical members of one of our in-house models (CNRM-CM5, hereafter CNRM).

ITV and DTR diagnostics require daily mean, maximum, and minimum 2m-temperatures (T, T^x, and T^n hereafter). Temperature observations over 1979–2008 are extracted from the E-OBS v8.0 gridded data set (0.25°×0.25°, hereafter EOBS) produced from in situ measurements provided by the ECA&D Project [*Haylock et al.*, 2008]. Monthly CMIP5 outputs related to hydrological cycle, energy fluxes, or atmospheric dynamics are also used for the investigation of physical processes underlying ITV and DTR changes. In order to ease the evaluation, observations and models are all interpolated onto a common horizontal grid before starting the analysis. As in *Cattiaux et al.* [2013a], the rather intermediate 256 × 128 grid of the CNRM model and a first-order conservative interpolation scheme are chosen. All regionally averaged statistics are computed over the Western Europe region defined as the land grid points within the box 5°W–25°E/42–55°N (drawn in Figure 1). Ultimately, all models have been taken with equal weights when computing ensemble statistics, despite some redundancies among originating groups or model components (Table S1).

2.2. Indices of Variability

As in *Kim et al.* [2013], the ITV is calculated as the average of absolute interdiurnal temperature differences (ITD) over a given number of days (n_d):

$$\mathrm{ITV} = \frac{1}{n_d - 1} \sum_{d=1}^{n_d-1} \left|\mathrm{ITD}_d\right| = \frac{1}{n_d - 1} \sum_{d=1}^{n_d-1} \left|T_{d+1} - T_d\right| \tag{1}$$

with T standing for the daily mean temperature, even if the interdiurnal variability of maximum and minimum temperatures (ITxV and ITnV) is briefly discussed in section 3. In this paper we compute the ITV for each summer ($n_d = 122$ days of JJAS) in order to derive a yearly index, and for 30 year periods ($n_d = 30 \times 122$). Note that the term *variability* arises in "ITV" because one can trivially show that ITD_d is related to the variance σ^2 of T over the 2 day interval $[\![d, d+1]\!]$ through:

$$\left|\mathrm{ITD}_d\right| = \left|T_{d+1} - T_d\right| = \sqrt{2}\,\sigma(T_{[\![d,d+1]\!]}) \tag{2}$$

so that averaging ITD_d over long periods of time can be interpreted as a measure of variability. The main advantage of using such day-to-day variations is that the ITV captures the short-term variability without being disturbed by longer-term variations such as the seasonal cycle and/or a multiyear trend, whereas traditional measures of variability (e.g., standard deviation and variance) would be. Despite this advantage, only a few studies have dealt with such indices of interdiurnal variability, one of the first being *Rosenthal* [1960].

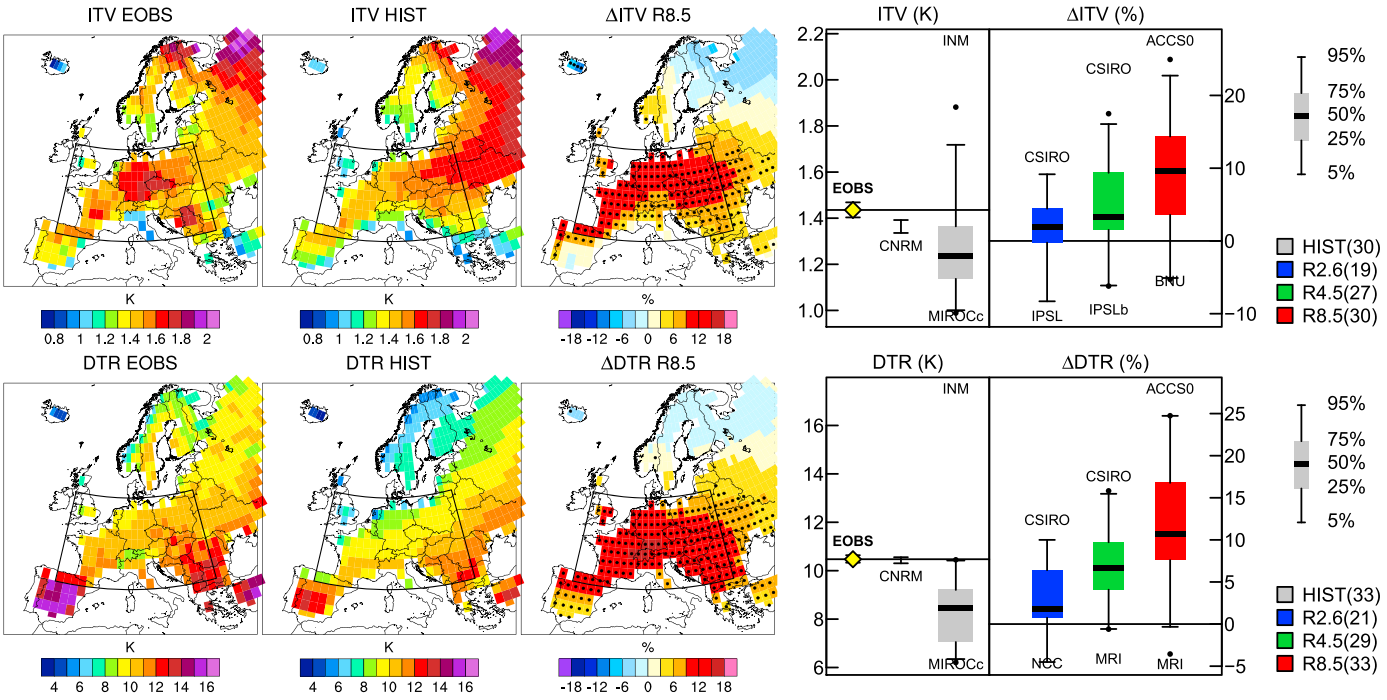

Figure 1. Present-day values and projected changes in mean (top row) ITV and (bottom row) DTR. Maps: EOBS values, ensemble mean present-day CMIP5 values, and ensemble mean RCP8.5 relative change (in %), with stippling for 75% model agreement with the sign of the ensemble mean. Graphs: individual values averaged over Western Europe (box in maps). EOBS estimate (yellow diamond and horizontal line), 10-member CNRM range (whisker) and present-day CMIP5 values (gray boxplot) in the leftmost graph. RCP2.6 (blue), RCP4.5 (green), and RCP8.5 (red) relative changes in the rightmost graph. See legend for boxplot signification and number of models included in each boxplot. The two extrema are explicited, and other outliers are indicated by dots. Ninety-five percent level confidence intervals estimated by bootstrap over years are added to EOBS estimates (very narrow).

The DTR is computed as the difference between daily maximum and minimum temperatures:

$$\mathrm{DTR}_d = T_d^x - T_d^n. \tag{3}$$

As for the ITV, the DTR can be averaged over each summer in order to derive a yearly index. Both indices can be computed for each grid point or for regionally averaged time series. Note that for ITV, the regional average of the index does not equal the index of the regional average, since modulus and sum are not commutable operations. Besides, ITV and DTR can be mixed in order to define an interdiurnal temperature range (ITR):

$$\mathrm{ITR}_d = \max\left(T_{d+1}^x - T_d^n, T_d^x - T_{d+1}^n\right), \tag{4}$$

which is briefly discussed in section 3 (the use of absolute values in the ITR definition is superfluous).

3. Results

3.1. Changes in Mean Day-to-Day and Diurnal Variations

Across Europe, the observed mean summer ITV ranges from about 1 to 2 K with important geographical discrepancies: the ITV is generally lower in coastal areas than inland (Figure 1, top row). Averaged over Western Europe, it reaches 1.4 K with maximum values at the intersection of Germany, Poland, and Czech Republic. Despite a fair representation of the land/sea contrast, CMIP5 models tend to slightly underestimate the ITV, except in Eastern Europe. The ensemble mean ITV over Western Europe is about 1.2 K, with individual model values ranging from 1 to 2 K. The effect of the internal variability, estimated either from a bootstrap procedure over the 30 yearly EOBS values or from the 10 CNRM runs (noticeably close to EOBS), appears rather weak on these 30 year and regional averages (~0.05 K). In all future scenarios, the European summer ITV is generally projected to increase. The ensemble mean increase in the RCP8.5 scenario reaches 15% in a band from the Western Pyrenees up to North-Eastern Germany. Individual

models even suggest 40% increases in some areas, while a few project a uniform reduction. Despite such discrepancies, more than 75% of models agree on the positive sign of the ITV response over Western Europe, thus suggesting a rather robust signal. This increase is even larger when considering maximal rather than mean temperatures (ITxV), while no clear signal occurs for ITnV (Figure S1).

The observed mean European summer DTR exhibits a strong meridional gradient, ranging from less than 10 K in Northern Europe to more than 15 K in Spain (Figure 1, bottom row), in line with the strong meridional gradient in solar downward radiation. On average, CMIP5 models uniformly underestimate the DTR by about 2 K, which is due to the combination of a warm bias in T^n and a cold bias in T^x [*Cattiaux et al.*, 2013a]. As for ITV, the effect of the internal variability ($\sim$ 0.3 K according to the EOBS bootstrapping or the CNRM ensemble, CNRM being again noticeably close to EOBS) appears small relative to the intermodel spread, from which the INM model stands out as a remarkable outlier (mostly because of a large cold T^n bias). Future projections suggest a generalized increase in DTR, with a robust model agreement over Western Europe. Maximum increases are projected over Switzerland and Southern Germany (more than 15%). Interestingly, the spatial pattern of the European DTR increase fairly resembles the ITV one, and there is a significant intermodel correlation between simulated ITV and DTR increases in highest scenarios (respectively, $r = 0.33$, 0.71, and 0.61 for RCP2.6, 4.5, and 8.5, only the last two being significant at 95%). This indicates that common physical processes may be involved over Europe, while ITV and DTR changes do not systematically coincide over other regions (e.g., U.S., Figure S1). Also, note that for both ITV and DTR, the projected changes are rather homothetic from one scenario to another (Figure S1). Finally, Figure S1 shows that the ITR behaves similarly to the DTR, so that we only focus on ITV and DTR in the following.

3.2. Changes in Distributions of Day-to-Day and Diurnal Variations

In order to further understand model biases and changes in European summer ITV, we compute the probability density functions (pdfs) of the day-to-day temperature differences (ITD) for both observations and models (Figure 2, top row). The Western Europe pdf is obtained as the average of grid point pdfs weighted by corresponding grid point areas (i.e., cosine of latitude). The observed ITD pdf is not centered on zero, as its mean corresponds to the average temperature difference between 30 September and 1 June (~ -2 K). As the median is closer to zero, the pdf is asymmetrical with a heavier tail in negative than in positive departures, as illustrated by a negative skewness. Although a detailed analysis is left for future studies, we speculate that a cloudy/rainy day after a few bright days may easily cool the surface while hot increments from one day to the next are more difficult to produce, since temperature generally builds up in the boundary layer through progressive continental heating by sensible heat fluxes [*Miralles et al.*, 2014]. While CMIP5 models reproduce this asymmetry fairly well, they tend to slightly underestimate the variance as well as the absolute value of the skewness and subsequently miss the amplitude of extreme ITD percentiles, especially the 1% quantile (negative ITD values). This is consistent with the slight underestimation of the ITV (recall that ITV $= \text{mean}_{d\in[\![1,n_d]\!]}\left(\left|\text{ITD}_d\right|\right)$). Future changes in the ITD pdf are characterized by increases in both variance and asymmetry, with a good model agreement. The general ITV increase found in Figure 1 is therefore associated with an increased frequency of extreme ITD values, especially negative ones: about 2% (2.5%) of RCP8.5 days are projected to witness ITD above (below) the present-day 99% (1%) quantile, rather than, by definition, 1% of days (Figure S2).

The shape of the DTR daily pdf is quite different from the ITD one, with a zero lower bound and a slightly positive skewness (Figure 2, bottom row). Interestingly, CMIP5 models simulate rather well both DTR variance and skewness, suggesting that the important underestimation of the mean DTR found in Figure 1 results from a general shift of the pdf toward smaller values (except for the INM model which simulates an unrealistic high DTR variance). The projected increase in mean DTR is associated with a decrease in skewness, while variance remains somewhat constant across scenarios. Hence, the major contribution to the mean DTR increase arises from moderate DTR values, even if extremely high DTR are also projected to increase. As an illustration, the present-day 99% quantile is projected to be exceeded up to 5% of the days in the RCP8.5 ensemble (Figure S2).

3.3. Drivers of Changes

Potential drivers of changes in ITV and DTR include the large-scale atmospheric dynamics, which is the main driver of surface temperature variability in Europe, and physical processes associated with the hydrological cycle and the modulation of the surface radiative budget (e.g., clouds). In order to estimate the contribution

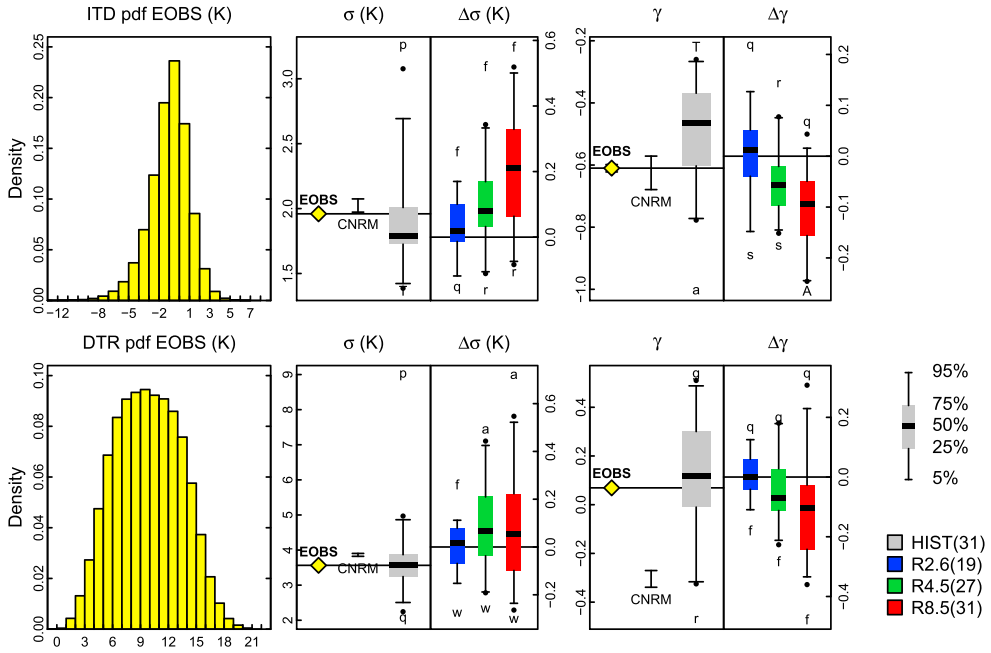

Figure 2. Biases and changes in (top row) ITD and (bottom row) DTR daily pdfs assessed from standard deviation (σ) and skewness (γ). Pdfs: EOBS densities averaged over Western Europe, estimated from 189 grid points × 3660 days (JJAS 1979–2008). The symbols σ and γ: EOBS value (yellow diamond and horizontal line), 10-member CNRM range (whisker), and present-day CMIP5 values (gray boxplot) in the leftmost graph; RCP2.6 (blue), RCP4.5 (green), and RCP8.5 (red) changes in the rightmost graph. See legend for boxplot signification and number of models included in each boxplot. The two extrema are explicited (see Table S1 for model symbols), and other outliers are indicated by dots.

of the former to projected increases in ITV and DTR, we use the weather regimes methodology proposed by *Cattiaux et al.* [2013b, hereafter CDP13], which is only briefly recalled here.

We consider the four North Atlantic weather regimes described in CDP13, which correspond to the preferred states of daily summer atmospheric circulations (Figure S3a). For each model, we break down the total changes Δ according to

$$\Delta = \delta_{\mathrm{WR}} + \delta_{\mathrm{NWR}} + \varepsilon\,, \tag{5}$$

with δ_{WR} the contribution of changes in frequencies and patterns of the weather regimes, δ_{NWR} the changes that would occur for unchanged circulations, and ε a residual term which we verify is systematically an order of magnitude smaller than the two others. Finally, as in CDP13, we evaluate the weather regime (WR) and nonweather regime (NWR) contributions to the ensemble dispersion in Δ by considering the quantities

$$\frac{\sigma_{\mathrm{WR}}}{\sigma_{\mathrm{WR}} + \sigma_{\mathrm{NWR}}} \quad \text{and} \quad \frac{\sigma_{\mathrm{NWR}}}{\sigma_{\mathrm{WR}} + \sigma_{\mathrm{NWR}}}, \tag{6}$$

with σ_{WR} (σ_{NWR}) the ensemble standard deviation of δ_{WR} (δ_{NWR}) terms. By construction, these two terms sum as 1 and provide relative estimates of WR and NWR contributions to the full model spread (ensemble standard deviation of Δ).

Despite noticeable and model-dependent changes in the frequencies of the regimes (Figure S3b), we find that both ITV and DTR increases, as well as their associated intermodel spreads, are dominated by the NWR contribution (Figure 3). The WR contribution is nevertheless important for the ITV; in particular, it explains up to 40% of the future spread (Figure 3). This methodology does not explicitly account for changes in day-to-day sequences of regimes (i.e., persistence or transition), possibly more relevant for the ITV, but Figure S3c shows that such changes are similar to changes in frequencies of occurrence.

Based on a subset of our CMIP5 ensemble, *Lindvall and Svensson* [2014] linked the European DTR increase to the concurrent drying of European soils, the reduction of cloud cover, and the decline in aerosols affecting

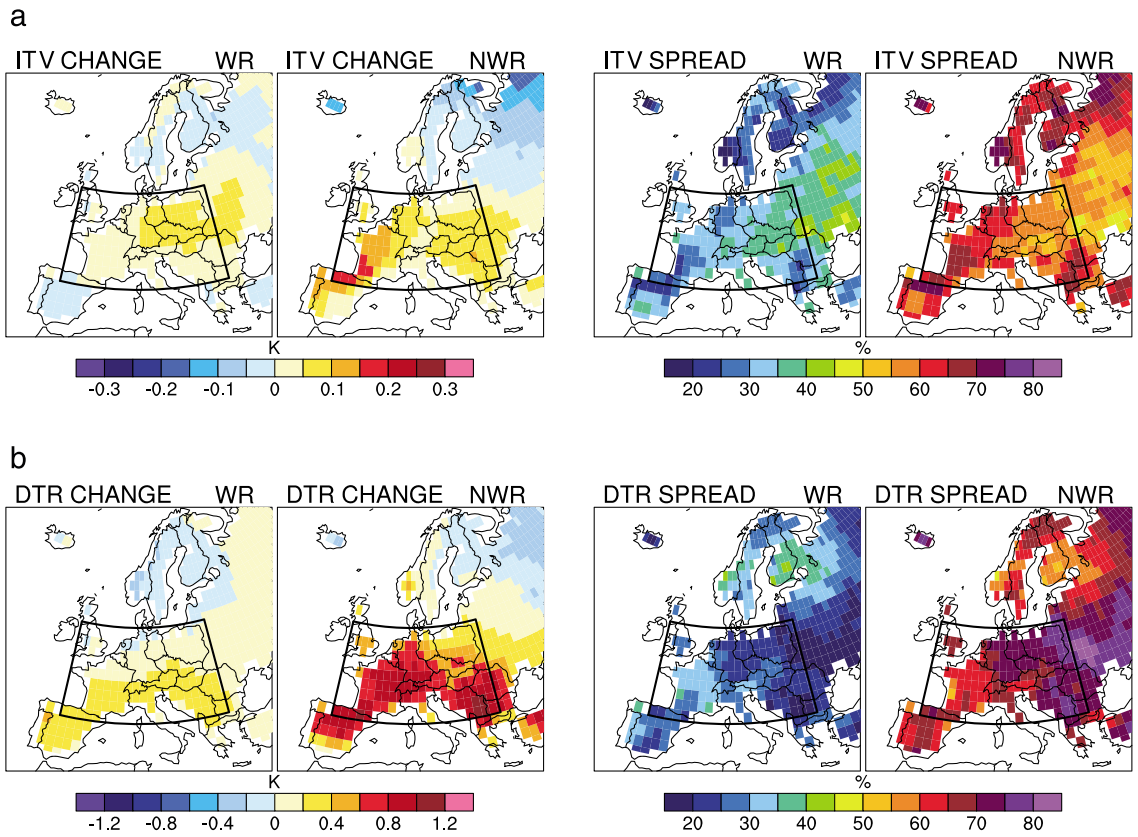

Figure 3. Dynamical versus nondynamical contributions to (a) ITV and (b) DTR changes and uncertainties in RCP8.5. (first and second columns) Ensemble means of weather regime (WR) and nonweather regime (NWR) contributions to ITV and DTR changes, estimated from equation (5). (third and fourth columns) Relative contributions of WR and NWR terms to the intermodel spread in ITV and DTR changes, estimated from equation (6) (the two contributions sum up to 100%).

the clear-sky downward solar radiation. Both soil moisture and cloud cover indeed tend to reduce the DTR: the former through the increased evaporative cooling, and the latter through the decreased daytime solar radiation and increased nighttime downward long-wave radiation. While we confirm the association of the DTR increase with the reduction in both the evaporative fraction (drying) and the surface cloud radiative effect (EF and CRE panels in Figure 4 (bottom)), we find no link with the decrease in aerosols (Figure S4). The latter is in line with the dominant effect of greenhouse gases found by *Lewis and Karoly* [2013] in 20th century trends but should be considered with caution given the lack of interactive aerosols in most CMIP5 models. The cloud influence is confirmed by significant links with the cloud cover, and splits equitably into short-wave and long-wave parts (Figure S4). Eventually, we find that changes in DTR are closely related to the mean temperature increase (Figure 3b), the correlation with the T^x increase being higher than with T^n (Figure S4).

Consistently with *Fischer and Schär* [2009] and *Fischer et al.* [2012], the ITV increase is found to be closely associated with the projected European drying (EF panel in Figure 4 (top)), while no significant correlation is found neither with mean warming (Figure 4), clouds or aerosols (Figure S4). We also find significant correlations in RCP2.6 and RCP4.5 with changes in the sea level pressure (SLP in Figure 4), confirming the substantial contribution of circulation changes to the ITV increase. While both ITV and DTR increases vary primarily as functions of the soil drying, underlying processes may differ as suggested by differences in correlations with hydrological variables in Figure S4. The ITV increase seems mainly driven by daytime processes (see ITxV and ITnV in Figure S1), therefore a stronger relationship with both latent heat flux and evaporative fraction. The DTR increase may also be modified by boundary layer nighttime processes, therefore a stronger relationship with the sensible heat flux.

The breakdown into weather regime and nonweather regime contributions in Figure 3 assumes that changes in weather regimes do not drive changes in physical variables used in Figure 4 and vice versa. This

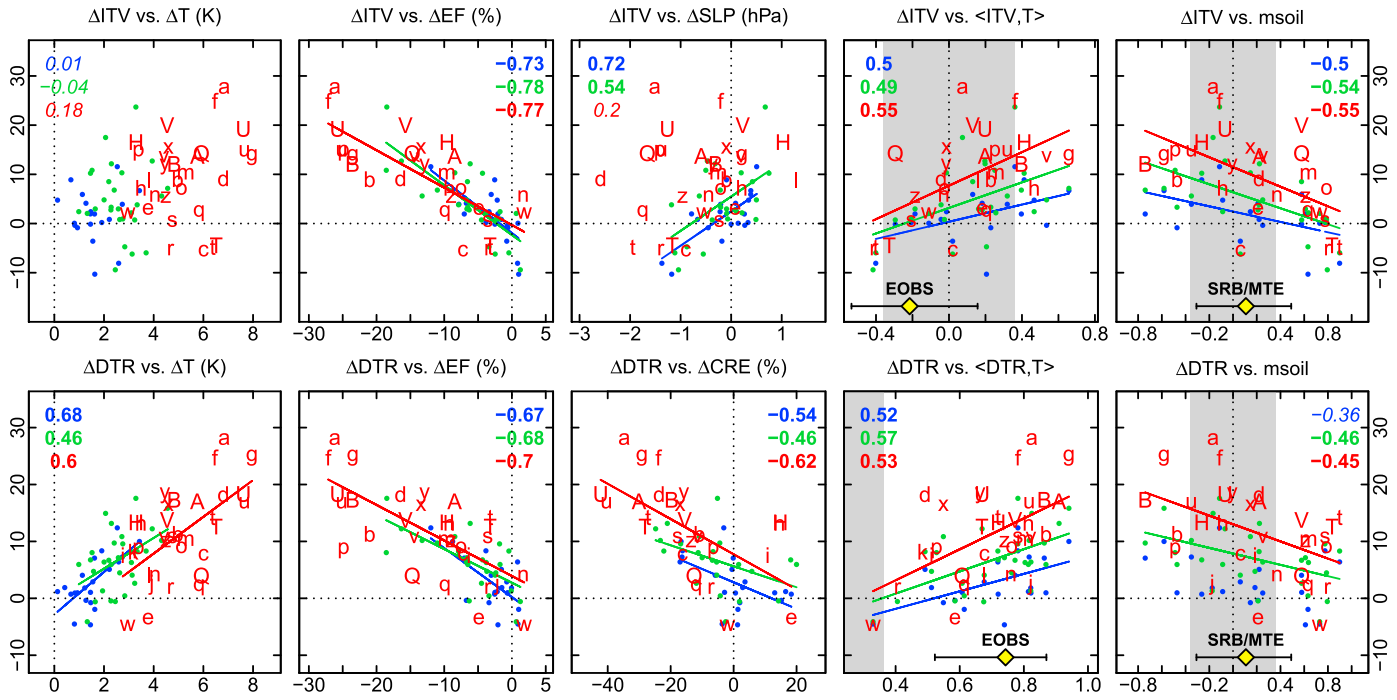

Figure 4. Drivers of changes and emerging constraints. (top) Projected change in ITV (in %) as a function of projected changes in temperature (*T*), evaporative fraction (EF), and sea level pressure (SLP); and present-day interannual correlations between ITV and temperature (<ITV, *T* >) and between latent heat flux and total downwelling radiation (*msoil*). (bottom) Same for DTR, except that SLP is replaced with surface cloud radiative effect (CRE). EF is defined as the ratio between latent heat flux and the sum of latent and sensible heat fluxes. CRE is defined as the difference between all-sky and clear-sky net surface radiation. Each symbol represents one model in one scenario (RCP2.6 in blue, RCP4.5 in green, and RCP8.5 in red), with models explicited by letters in RCP8.5 (see Table S1). For each scenario, regression lines are added when 95% significant, and correlation coefficients are indicated (bold when 95% significant, otherwise italics). On the fourth and fifth columns, observational estimates of *x* values are indicated by yellow diamonds and 95% level confidence interval (see details in text); the range of non-95%-significant *x* values according to a two-tailed *t* test with 28 degrees of freedom (30 years) is shaded in gray.

assumption seems reasonable since (i) the large spatial domain used for weather regimes, the location of their centers of action, and the strong internal variability prevent them to be substantially affected by local European variables, and (ii) if changes in European evaporative fraction and cloudiness were circulation driven, then weather regime contributions in Figure 3 would be much greater.

3.4. Emerging Constraints From the 1979–2008 Period

An interesting question is whether both ITV and DTR projected increases can be related to mean values, trends, and/or interannual correlations over 1979–2008 in CMIP5 models, enabling the possibility of constraining model projections by observations [e.g., *Stegehuis et al.*, 2013]. For both indices, no relationship is found between projected increases and present-day biases, and the strongest potential constraints arise from interannual correlations (Figure S4). For example, the greatest ITV and DTR increases are found for the models for which these indices are the more correlated to the mean temperature over 1979–2008 (<ITV, *T* > and <DTR, *T* > in Figure 4). While the <DTR, *T* > correlation is statistically significant in EOBS, the <ITV, *T* > relationship is less clear (even a negative ITV trend is observed over 1979–2008). Such 30 year correlations are strongly sensitive to the internal variability, as evidenced by 95% level confidence intervals associated with the correlation test, thus limiting the possibility of constraining future projections.

Beyond the link between indices of variability and mean temperature, potential constraints may arise from physical drivers identified in section 3.3. For example, both ITV and DTR are found negatively correlated with the evaporative fraction at the interannual timescale over 1979–2008 (not shown), and the higher the amplitude of the correlation, the higher the projected ITV and DTR change (Figure S4). This is supported by the relationship between present-day drying trends and ITV and DTR changes (Figure S4). Conversely, no such potential constraints are found with cloud processes and large-scale dynamics (Figure S4).

Finally, the two metrics considered by *Boé and Terray* [2014] as relevant for reducing uncertainties in summer European climate change are tested: the present-day interannual correlations between (i) surface latent

heat flux and total downwelling radiation (hereafter m_{soil}) and (ii) cloud cover and surface temperature (m_{cloud}). The former indicates whether the evapotranspiration is limited by the available energy ($m_{soil} > 0$) or the available soil moisture ($m_{soil} < 0$), while the latter, generally negative, is a simple indicator of cloud-temperature interactions. In CMIP5 models, while no robust link appears between m_{cloud} and ITV and DTR changes, we find that the more the evapotranspiration is limited by the soil moisture in the present-day climate, the stronger the projected drying and the ITV and DTR increases (m_{soil} in Figure 4). The observational estimate of *msoil*, which we derive from the GEWEX SRB downwelling radiation (http://www.gewex.org/srbdata.htm, only covering the 1984–2007 period) and the MTE surface latent heat flux (https://www.bgc-jena.mpg.de/bgi), is slightly positive, albeit associated with a large confidence interval.

4. Summary and Conclusions

This paper investigates the future increases in both interdiurnal and diurnal variations of European summer temperatures (ITV and DTR) projected by the CMIP5 ensemble. We find that the mean ITV increase is due to a widening of the asymmetric pdf of day-to-day temperature differences (ITD), while the mean DTR increase rather arises from both a translation and an enhanced skewness of its pdf. Consequently, on average over the model ensemble, extreme ITD and DTR values are expected to occur more frequently by the end of the 21st century. Processes underlying these changes in CMIP5 projections include the summer drying over Europe for both indices, the reduction in cloud cover for the DTR, and the changes in large-scale dynamics for the ITV. Decreases in both surface evaporative fraction and cloud radiative effect are stronger in Europe compared to other regions of the Northern midlatitudes, which may explain why ITV and DTR increases specifically concern Europe (Figure S5). Further work, possibly involving targeted model experiments, is nevertheless required to more precisely quantify the contributions of dynamical and nondynamical processes, and their nonlinear interactions (e.g., horizontal advection), to ITV and DTR increases.

While most of the models agree on the positive sign of European ITV and DTR changes, which itself constitutes a relevant information for impact communities, strong uncertainties remain on the amplitude. For a given scenario, the possibility of reducing the model spread on the basis of present-day metrics is investigated. We find that models simulating the highest ITV and DTR future increases tend to have (i) positive correlations between ITV and DTR and the mean temperature and (ii) their evapotranspiration limited by the soil moisture in the present-day climate. Observational estimates suggest that future ITV and DTR increases may, respectively, lie in the lower half and the middle of the model spread, although this assessment is highly sensitive to the internal variability. A better estimation of present-day trends in ITV and DTR, e.g., through data homogeneization and/or detection and attribution studies [*Hanlon et al.*, 2013; *Lewis and Karoly*, 2013], and a better understanding of processes underlying interannual variations of ITV and DTR, e.g., through sensitivity experiments to soil moisture [*Zampieri et al.*, 2009], could be helpful in reducing the uncertainties in future changes in the variability of European summer temperatures.

Acknowledgments
We greatly thank Erich Fischer and one anonymous reviewer for helpful comments that helped improving the manuscript. We also thank R. Vautard (LSCE) and J. Najac (EDF) for fruitful discussions, as well as S. Tyteca (CNRM-GAME) for data handling. We acknowledge the World Climate Research Programme's Working Group on Coupled Modelling, which is responsible for CMIP, and we thank the climate modeling groups (listed in Table S1 of this paper) for producing and making available their model output (http://pcmdi9.llnl.gov/esgf-web-fe/). We acknowledge the E-OBS data set from the EU-FP6 project ENSEMBLES and the data providers in the ECA&D project (http://www.ecad.eu). This work was supported by the Climate-KIC E3P and the EU-FP7 EUCLIPSE projects.

The Editor thanks Erich Fischer and an anonymous reviewer for their assistance in evaluating this paper.

References

Boé, J., and L. Terray (2014), Land–sea contrast, soil-atmosphere and cloud-temperature interactions: Interplays and roles in future summer European climate change, *Clim. Dyn.*, *42*(3–4), 683–699, doi:10.1007/s00382-013-1868-8.

Cattiaux, J., P. Yiou, and R. Vautard (2012), Dynamics of future seasonal temperature trends and extremes in Europe: A multi-model analysis from CMIP3, *Clim. Dyn.*, *38*(9–10), 1949–1964, doi:10.1007/s00382-011-1211-1.

Cattiaux, J., H. Douville, and Y. Peings (2013a), European temperatures in CMIP5: Origins of present-day biases and future uncertainties, *Clim. Dyn.*, *41*(11–12), 2889–2907, doi:10.1007/s00382-013-1731-y.

Cattiaux, J., H. Douville, A. Ribes, F. Chauvin, and C. Plante (2013b), Towards a better understanding of changes in wintertime cold extremes over Europe: A pilot study with CNRM and IPSL atmospheric models, *Clim. Dyn.*, *40*(9–10), 2433–2445, doi:10.1007/s00382-012-1436-7.

Fischer, E., and C. Schär (2009), Future changes in daily summer temperature variability: Driving processes and role for temperature extremes, *Clim. Dyn.*, *33*(7), 917–935, doi:10.1007/s00382-008-0473-8.

Fischer, E., J. Rajczak, and C. Schär (2012), Changes in European summer temperature variability revisited, *Geophys. Res. Lett.*, *39*, L19702, doi:10.1029/2012GL052730.

Hanlon, H., S. Morak, and G. Hegerl (2013), Detection and prediction of mean and extreme European summer temperatures with a multimodel ensemble, *J. Geophys. Res. Atmos.*, *118*(17), 9631–9641, doi:10.1002/jgrd.50703.

Haylock, M., N. Hofstra, A. Klein Tank, E. Klok, P. Jones, and M. New (2008), A European daily high-resolution gridded data set of surface temperature and precipitation for 1950–2006, *J. Geophys. Res.*, *113*, D20119, doi:10.1029/2008JD10201.

Kim, O.-Y., B. Wang, and S.-H. Shin (2013), How do weather characteristics change in a warming climate?, *Clim. Dyn.*, *41*(11–12), 3261–3281, doi:10.1007/s00382-013-1795-8.

Kjellström, E., L. Bärring, D. Jacob, R. Jones, G. Lenderink, and C. Schär (2007), Modelling daily temperature extremes: Recent climate and future changes over Europe, *Clim. Change*, *81*(Suppl 1), 249–265, doi:10.1007/s10584-006-9220-5.

Lewis, S., and D. Karoly (2013), Evaluation of historical diurnal temperature range trends in CMIP5 models, *J. Clim.*, *26*(22), 9077–9089, doi:10.1175/JCLI-D-13-00032.1.

Lindvall, J., and G. Svensson (2014), The diurnal temperature range in the CMIP5 models, *Clim. Dyn.*, 1–17, doi:10.1007/s00382-014-2144-2.

Lobell, D. (2007), Changes in diurnal temperature range and national cereal yields, *Agric. For. Meteorol.*, *145*(3), 229–238, doi:10.1016/j.agrformet.2007.05.002.

Miralles, D., A. Teuling, C. van Heerwaarden, and J.-G. de Arellano (2014), Mega-heatwave temperatures due to combined soil desiccation and atmospheric heat accumulation, *Nat. Geosci.*, *7*, 345–349, doi:10.1038/ngeo2141.

Parey, S., D. Dacunha-Castelle, and T. Hoang (2010), Mean and variance evolutions of the hot and cold temperatures in Europe, *Clim. Dyn.*, *34*(2–3), 345–359, doi:10.1007/s00382-009-0557-0.

Parey, S., T. Hoang, and D. Dacunha-Castelle (2013), The importance of mean and variance in predicting changes in temperature extremes, *J. Geophys. Res. Atmos.*, *118*(15), 8285–8296, doi:10.1002/jgrd.50629.

Rosenthal, S. (1960), The interdiurnal variability of surface-air temperature over the North Atlantic Ocean, *J. Meteorol.*, *17*(1), 1–7.

Schär, C., P. Vidale, D. Luethi, C. Frei, C. Haeberli, M. Liniger, and C. Appenzeller (2004), The role of increasing temperature variability in European summer heatwaves, *Nature*, *427*(6972), 332–336, doi:10.1038/nature02300.

Seneviratne, S., D. Luethi, M. Litschi, and C. Schär (2006), Land-atmosphere coupling and climate change in Europe, *Nature*, *443*(7108), 205–209, doi:10.1038/nature05095.

Sillmann, J., V. Kharin, F. Zwiers, X. Zhang, and D. Bronaugh (2013), Climate extremes indices in the CMIP5 multimodel ensemble: Part 2. Future climate projections, *J. Geophys. Res. Atmos.*, *118*, 2473–2493, doi:10.1002/jgrd.50188.

Stegehuis, A., R. Vautard, P. Ciais, A. Teuling, M. Jung, and P. Yiou (2013), Summer temperatures in Europe and land heat fluxes in observation-based data and regional climate model simulations, *Clim. Dyn.*, *41*(2), 455–477, doi:10.1007/s00382-012-1559-x.

Yiou, P., D. Dacunha-Castelle, S. Parey, and T. Huong Hoang (2009), Statistical representation of temperature mean and variability in Europe, *Geophys. Res. Lett.*, *36*, L04710, doi:10.1029/2008GL036836.

Zampieri, M., F. D'Andrea, R. Vautard, P. Ciais, N. de Noblet-Ducoudré, and P. Yiou (2009), Hot European summers and the role of soil moisture in the propagation of Mediterranean drought, *J. Clim.*, *22*, 4747–4758, doi:10.1175/2009JCLI2568.1.